Metal Ceramics

International Edition: DOI: 10.1002/anie.201814128
German Edition: DOI: 10.1002/ange.201814128

A Series of MAX Phases with MA-Triangular-Prism Bilayers and Elastic Properties

*Hongxiang Chen, Dongliang Yang, Qinghua Zhang, Shifeng Jin, Liwei Guo, Jun Deng, Xiaodong Li, and Xiaolong Chen**

Abstract: *We report a new type of MAX phase (M = transition metals, A = main group elements, and X = C/N), Nb_3As_2C, designated as 321 phase. It differs from all the previous $M_{n+1}AX_n$ phases in that it consists of an alternate stacking of one MX layer and two MA layers in its unit cell, while only one MA layer is allowed in usual MAX phases. The new 321 phase exhibits a bulk modulus of Nb_3As_2C up to 225(3) GPa as determined by high-pressure synchrotron X-ray diffraction, one of the highest values among MAX phases. Isostructural 321 phases V_3As_2C, Nb_3P_2C, and Ta_3P_2C are also found to exist. First-principles calculations reveal the outstanding elastic stiffness in 321 phases. Among all 321 phases, Nb_3P_2C is predicted to have the highest elastic properties. These 321 phases, represented by a chemical formula $M_{n+1}A_nX$, were added as new members to the MAX family and their other properties deserve future investigations.*

MAX phases[1] belong to a family of non-van-der-Waals-type layered compounds with a general formula of $M_{n+1}AX_n$ ($n = 1, 2, 3$) in which M = transition metals, A = main group elements, and X = C/N. MAX phases are also termed as metallic ceramics[2] for their combined characteristic properties of both ceramics and metals. Some of them host high thermal and electrical conductivity, good elastic performance, excellent resistance to corrosion, oxidation, and thermal shock, easy machinability and unusual damage-tolerance.[2a,3] These combined elastic, electrical and thermal properties enable them to be promising materials for various applications,[4] especially in the structural or conductive components under high temperatures. Besides, MAX phases also have drawn much attention as the precursor of MXenes.[5] Owing to the relatively weak bonding of M–A in MAX phases, a series of two dimensional transition-metal carbides can be obtained from acid etching of selected MAX phases.[6]

The study of MAX phases started from 1960s when the H-phases were found by Nowotny's group.[7] Now, over 60 MAX phases are found. Depending on the value of n, the M_2AX, M_3AX_2, and M_4AX_3 phases are usually named as 211, 312, and 413 phases, respectively.[1b] The crystal structures of MAX phases usually share a common symmetry with space group $P6_3/mmc$. Each X atom is coordinated by six M atoms forming an octahedron, and each M atom by six A atoms forming a hexagonal prism as shown in Figure 1. $M_{n+1}AX_n$ can be regarded as an alternate stacking of n MX layers consisting of the edge-shared M_6X octahedrons and one MA layer consisting of edge-shared M_6A triangular prisms. It should be

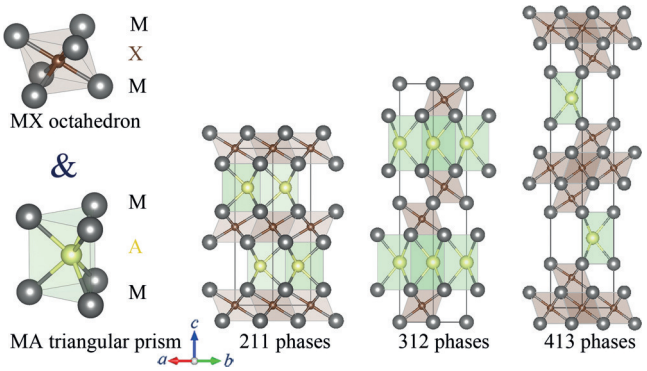

Figure 1. The crystal structure of $M_{n+1}AX_n$ phases. Schematic representation of the M_6X octahedron and M_6A triangular prism in MAX phases, and the crystal structure of 211, 312, and 413 phases viewed from [110] direction.

[*] Dr. H. Chen, Dr. Q. Zhang, Dr. S. Jin, Prof. Dr. L. Guo, J. Deng, Prof. Dr. X. Chen
Research & Development Center for Functional Crystals, Laboratory of Advanced Materials and Electron Microscopy, Beijing National Laboratory for Condensed Matter Physics, Institute of Physics
Chinese Academy of Sciences
Beijing 100190 (China)
E-mail: chenx29@iphy.ac.cn

Dr. H. Chen
School of Materials Science and engineering
Fujian University of Technology
Fuzhou 350118 (China)

Dr. D. Yang, Prof. Dr. X. Li
Beijing Synchrotron Radiation Facility, Institute of High Energy Physics, Chinese Academy of Science
Beijing 100049 (China)

J. Deng, Prof. Dr. X. Chen
School of Physical Sciences
University of Chinese Academy of Sciences
Beijing 101408 (China)

Prof. Dr. X. Chen
Collaborative Innovation Center of Quantum Matter
Beijing 100084 (China)

Prof. Dr. L. Guo
Center of Materials Science and Optoelectronics Engineering
University of Chinese Academy of Sciences
Beijing 100049 (China),
and
Songshan Lake Materials Laboratory
Dongguan, Guangdong 523808 (China)

Supporting information and the ORCID identification number(s) for the author(s) of this article can be found under: https://doi.org/10.1002/anie.201814128.

noted that two and three MX layers can be combined into edge-shared bilayer and trilayer as in 312[8] and 413[9] phases, respectively. Besides, Mo_2Ga_2C,[10] Ta_2S_2C, Ta_2Se_2C,[11] and Nb_2S_2C,[12] named as 221 phases, also have a similar structure with $M_{n+1}AX_n$ phases, where two layers of A atoms exist between the MX layers. The multi-layering of MA layers, however, has never been found among the known MAX phases.

Herein, we report new MAX phases in As-, P- containing systems, namely, Nb_3As_2C, V_3As_2C, Nb_3P_2C, and Ta_3P_2C. Their crystal structures are determined by X-ray diffraction (XRD) and high resolution transmission electron microscopy (HRTEM). These isostructural phases can be regarded as formation from the alternate stacking of one MX layer and two MA layers in their unit cell. They can be expressed as $M_{n+1}A_nX$ ($n=2$), henceforth referred to as 321 phases. In contrast to the known MAX phases, the multi-layered MA layer is first observed in 321 phases. The pure phase of Nb_3As_2C was obtained by an optimized synthesis process. It is found that Nb_3As_2C has a bulk modulus up to 225(3) GPa as revealed by high pressure synchrotron XRD (HPXRD) study with pressure up to 47 GPa, which is confirmed by the results from the first-principles calculations. These 321 phases form a new class of the MAX family.

The 321 phases were synthesized by a two-step process. Take Nb_3As_2C as an example, the process is illustrated in Figure 2a. High purity Nb, As and graphite powders were mixed and sealed in an evacuated quartz tube, then heating the quartz tube to 850 °C in 20 hours, and kept for 10 hours. The main by-products are NbAs, Nb, and graphite as revealed by XRD (see Figure S1 in the Supporting Information). Secondly, the as-prepared powder was pulverized, pelletized, sealed in a quartz tube, and heated to 1280 °C in 8 hours and kept for 15 hours. The end-product is Nb_3As_2C with grain size 2–10 μm (Figure S2). The elemental composition determined by inductively coupled plasma-atomic emission spectrometry is Nb:As:C = 2.9:1.9:1, very close to the nominal composition. We found that long-time sintering around 1000 °C always leads to the formation of Nb_2AsC (see Figure S3), and we cannot obtain 321 phase with further sintering at 1280 °C. Thermodynamic calculations (see Figure 2b) indicate the reaction path $Nb_2AsC + NbAs = Nb_3As_2C$ is unfavored as the free energy (ΔF) is positive. In comparison, the free energy for the reaction NbAs + Nb + C = Nb_3As_2C is negative, meaning that this path is possible. The differential thermal analysis (see Figure 2c) confirms this. An exothermic peak at 1260 °C should be an indication of the reaction temperature, in agreement with our synthetic temperature. It is noted that Nb_3As_2C will decompose under high vacuum when the sample was heated up to about 1600 °C (see Figure S4).

All peaks in the powder XRD pattern can be well indexed as $a = 3.36056(6)$ Å, and $c = 18.69508(35)$ Å with space group No. 194, $P6_3/mmc$ as shown in Figure 3a. The crystal structure of Nb_3As_2C was solved by direct method using EXPO2014 program suite.[13] The Rietveld refinements converge to the agreement factors $R_p = 4.11\,\%$ and $R_{wp} = 5.45\,\%$. The atom positions of 321 phases are listed in Table S1. For Nb_3As_2C, $z_M = 0.05951(4)$, $z_A = 0.15849(5)$.

As shown in Figure 3b, the crystal structure of Nb_3As_2C exhibits distinct structural features from the conventional $M_{n+1}AX_n$ phases. There are two Nb positions in Nb_3As_2C in the unit cell, as labeled by Nb1 and Nb2. Each As atoms is coordinated by three Nb1 atoms and three Nb2 atoms forming a triangular prism; Each C atom is coordinated by six Nb1 atoms forming an octahedron. Different from $M_{n+1}AX_n$ phases, the MA-triangular-prism layers here are bilayers. The crystal structure of Nb_3As_2C could be seen as an

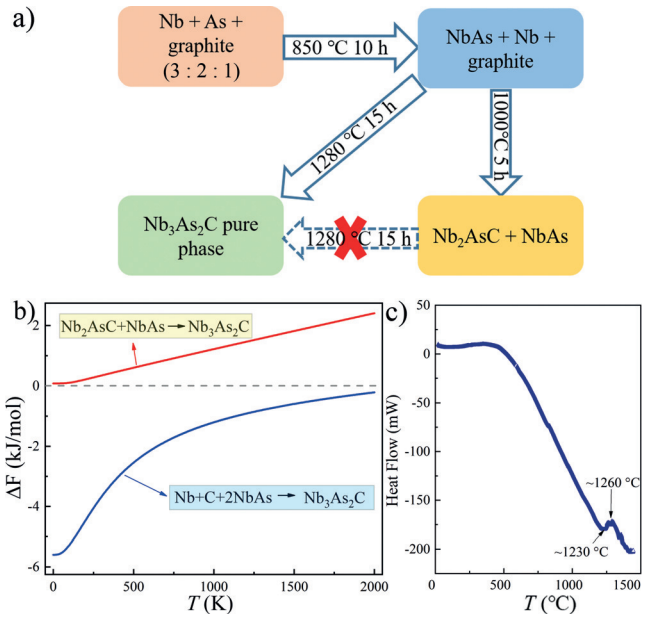

Figure 2. The synthesis of Nb_3As_2C phase. a) The synthetic process of Nb_3As_2C. b) The theoretical free energy of two reaction paths. c) Differential thermal analysis of 850 °C sintered sample (NbAs + Nb + C).

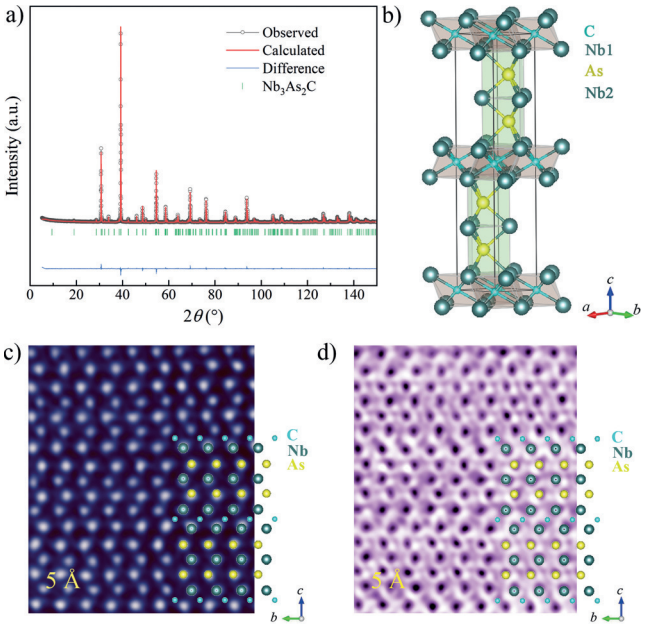

Figure 3. Crystal structure of Nb_3As_2C. a) The Rietveld refinement of the XRD data of Nb_3As_2C. b) The crystal structure of Nb_3As_2C. c) The HADDF image of the atomic arrangement of Nb_3As_2C viewed from [100] direction. d) The ABF image.

alternate stacking of MX-octahedron layer and MA-triangular-prism bilayer. Similar to most MAX phases, the Nb, As, and C atoms of 321 phases are all in hexagonal closed packing positions.

The atomic arrangement in the unit cell was examined by high-angle annular dark-field (HAADF) and annular-bright-field (ABF) scanning transmission electron microscopy (STEM) as shown in Figure 3c,d. The atomic stacking of Nb and As atoms along the [001] direction were clearly observed in HAADF and ABF images, matching well with the solved structure. Due to the low contrast of C atoms, it is hard to observe the C atoms[14] in HADDF image. But in ABF image, C atoms can be identified lying in between the Nb atom layers. The atomically resolved HAADF and ABF images justify the reliability of the solved structure.

For Nb_3As_2C, $d_{Nb1\text{-}C} = 2.2365$ Å is slightly shorter than the $d_{Nb\text{-}C} = 2.2422$ Å; the average of $d_{Nb1\text{-}As}$ (2.6814 Å) and $d_{Nb2\text{-}As}$ (2.5867 Å) is close to the $d_{Nb\text{-}As}$ (2.6343 Å) in Nb_2AsC. This suggests the strong Nb-C and Nb-As bonding in Nb_3As_2C as the case in Nb_2AsC. The strong bonding strengths in this 321 phase are expected to exhibit high elastic performance as in As-, P-, S-containing 211 phases.[15]

HPXRD under pressures of up to 47 GPa were applied to determine the bulk modulus of Nb_3As_2C. As shown in Figure 4a, no new peak appears with the increasing pressure, indicating the excellent stability of Nb_3As_2C under high pressures. The strongest three peaks (105), (100), and (110) can be obviously seen to shift to high angles with increasing pressures. The pressure dependence of the normalized lattice parameters a/a_0, c/c_0 are shown in Figure 4b. Similar to the case with Zr_2SC,[15d] the compressibility of this 321 phase are quite isotropic, while are strong anisotropic[16] for most MAX phases. Both a and c shrink by less than 6%, and the cell volume by about 16% at the pressure of 47 GPa. The pressure-dependent V/V_0 can be well fitted by the Birch-Murnaghan[17] equation of state with a correlation coefficient $R^2 = 0.9987$, [Eq. (1)]

$$P = 3/2B_0[(V/V_0)^{-7/3} - (V/V_0)^{-5/3}] \times \{1 + \frac{3}{4}(B_0' - 4)(V/V_0)^{-2/3} - 1\} \quad (1)$$

where B_0 is the bulk modulus and B_0' its first pressure derivative. The fitted B_0 and B_0' are 225(3) GPa, and 2.6-(3) GPa, respectively. The value of B_0 of Nb_3As_2C is nearly equal to the $B_0 = 224(2)$ GPa for Nb_2AsC,[15b] and quite close to the highest $B_0 = 261(2)$ GPa for β-Ta_4AlC_3.[18] This result shows that the existence of more Nb–As bonds in Nb_3As_2C does not cause a decrease in bulk modulus, which provide further evidence of that the M–A bonding and M–X bonding are close in strength in the As-containing MAX phases.

First-principles calculations have been used to evaluate the elastic constants c_{ij} of most MAX phases within an accuracy of about 10%.[19] We performed the first-principles calculations of the elastic constants of Nb_3As_2C along with other 321 phases. For hexagonal symmetry, there are five independent elastic constants: c_{11}, c_{12}, c_{13}, c_{33}, and c_{44}

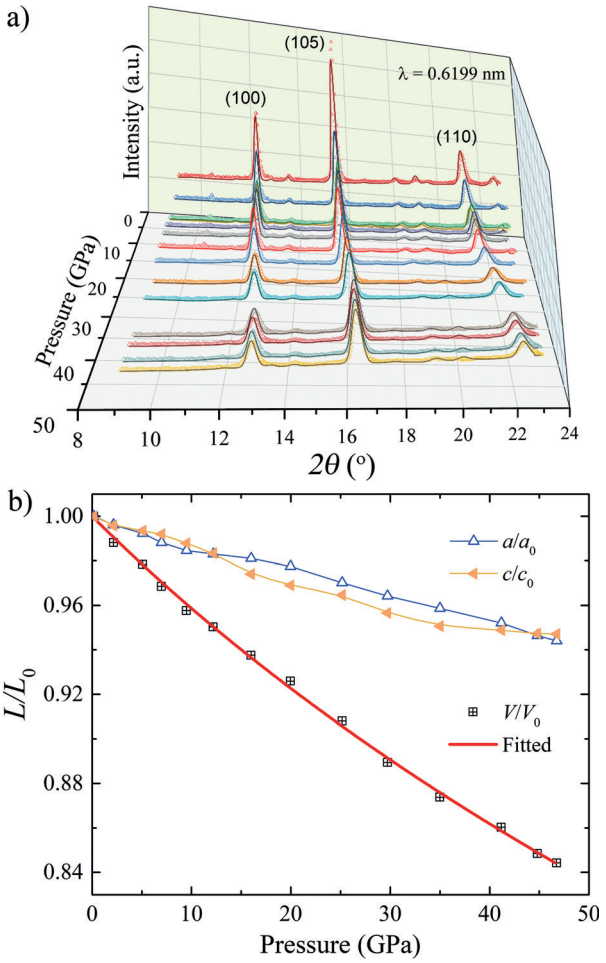

Figure 4. High-pressure XRD study of Nb_3As_2C. a) The pressure dependence of the XRD patterns of Nb_3As_2C, the solid lines are the results of refinements. b) Pressure-dependent relative cell parameters (a/a_0, c/c_0, and V/V_0). The red curve is the fit to data by the Birch-Murnaghan equation of state.

as shown in the Equation S1.[19] The calculated elastic constants c_{ij} are listed in Table S2. The bulk modulus B_V, Young's modulus E_V, shear modulus G_V and Poisson ratio ν as listed in Table 1 were then calculated by the Voigt method using Equations S2–S5.[19] The Poisson ratio ν of 321 phases are in the range of 0.22–0.24. For Nb_3As_2C, the bulk modulus B_V is 198.3 GPa. The calculated B_V for Nb_2AsC by the same method is near 200 GPa, consistent with the results 204 GPa calculated by Mekour et al.[20] Accordingly, the ab initio calculations tend to underestimate the elastic properties of As-, P- containing MAX phases. The elastic modulus and shear modulus of Nb_3As_2C ($E_V = 306.5$ GPa, $G_V = 123.4$ GPa)

Table 1: The theoretical lattice parameters a' and c' and elastic parameters of 321 phases.

Phase	a' [Å]	c' [Å]	G_V [GPa]	E_V [GPa]	B_V [GPa]	ν
Nb_3As_2C	3.3857	18.9088	123.4	306.5	198.3	0.24
Nb_3P_2C	3.3334	18.2091	152.0	371.8	223.6	0.22
Ta_3P_2C	3.3128	18.1167	149.0	365.3	222.0	0.23
V_3As_2C	3.1657	17.8618	121.4	297.8	181.2	0.23

are slightly smaller than Nb_2AsC (E_V = 313 GPa, G_V = 126 GPa).[21]

As shown in Table 1, the bulk modulus of Nb_3P_2C and Ta_3P_2C are 223.6 GPa and 222.0 GPa, respectively. Because of the underestimation of the bulk modulus in the case of Nb_3As_2C, the experimental bulk modulus of Nb_3P_2C and Ta_3P_2C might be higher than that for Nb_3As_2C. It can be seen that the P-containing 321 phases are better elastically performed than As-containing 321 phases. Nb_3P_2C (E_V = 371.8 GPa, G_V = 152.0 GPa) performed best among 321 phases, even better than the calculated results in Nb_2PC (E_V = 333 GPa and G_V = 134 GPa).[21] More interestingly, the calculated results of Nb_3P_2C also higher than the experimental results in Nb_4AlC_3, which are the best values among the MAX phases (E_V = 365 GPa, G_V = 149 GPa parallel to basal plane, and E_V = 353 GPa, G_V = 153 GPa vertical to basal plane).[22] Considering the possible best elastic performance, relatively low theoretical density and low toxicity, Nb_3P_2C is a more promising material for application among these 321 phases.

Until now, the known As- or P- containing conventional MAX phases include Nb_2AsC, Nb_2PC, V_2AsC, and V_2PC.[7,23] The synthesis of other As- or P- containing 321 phases Ta_3P_2C, Nb_3P_2C and V_3As_2C were tried. We find these phases exist but the secondary phases MX, M_2AX or MA are often present. For instance, the main phase Nb_3P_2C content is 57.7(6) mol%, and the secondary phases are NbC (5.2(1)%), Nb_2PC (22.7-(2)%), NbP (14.4(2)%), see Figure S5. The Rietveld refinements were performed for Nb_3P_2C and Ta_3P_2C samples. For V_3As_2C, there are many unknown peaks in the PXRD pattern as shown in Figure S6, so we only indexed the peaks belonging to V_3As_2C to obtain its lattice parameters. The lattice parameters, atomic positions, phase content, and agreement factors of 321 phases are listed in Table S1. The structural information including the bond lengths and bond angles are listed in Table S3.

In conclusion, a new series of MAX phases, Nb_3As_2C, V_3As_2C, Nb_3P_2C, and Ta_3P_2C, named as 321 phases, were added to the family of MAX phases. With the optimized synthesis method, pure phases of Nb_3As_2C can be obtained, and we suggest the reaction path should follow $2NbAs + Nb + C \rightarrow Nb_3As_2C$. XRD and TEM results revealed that the 321 phases share common symmetry and constituent units with the conventional $M_{n+1}AX_n$ phases. The structure of 321 phases consists of alternate stacking of MX-octahedron layers and MA-triangular-prism bilayers. The First-principles calculations and HPXRD reveal the outstanding elastic performance of 321 phases. The experimental bulk modulus of Nb_3As_2C is up to 225(3) GPa, which is close to the highest values among MAX phases. The predicted the elastic stiffness (E_V = 371.8 GPa, G_V = 152.0 GPa, B_V = 223.6 GPa), relative low density and low toxicity of Nb_3P_2C make it a most promising material for future application. These 321 phases are the first series of MAX phases that can be expressed as $M_{n+1}A_nX$ with $n > 1$. Their novel structure and outstanding elastic stiffness in 321 phases are interesting, which is encouraging to search for new $M_{n+1}A_nX$ phases.

Acknowledgements

This work is financially supported by the National Natural Science Foundation of China under granting numbers: No. 51532010, No. 91422303; the Key Research Program of Frontier Sciences, CAS, Grant No. QYZDJ-SSW-SLH013; and the Strategic Priority Research Program of Chinese Academy of Sciences (Grant No. XDB07020100).

Conflict of interest

The authors declare no conflict of interest.

Keywords: carbides · elastic constants · high pressure XRD · layered compounds · MAX phases

How to cite: *Angew. Chem. Int. Ed.* **2019**, *58*, 4576–4580
Angew. Chem. **2019**, *131*, 4624–4628

[1] a) M. W. Barsoum, T. El-Raghy, *Am. Sci.* **2001**, *89*, 334–343; b) M. W. Barsoum, *Prog. Solid State Chem.* **2000**, *28*, 201–281; c) P. Eklund, M. Beckers, U. Jansson, H. Högberg, L. Hultman, *Thin Solid Films* **2010**, *518*, 1851–1878.

[2] a) Z. M. Sun, *Int. Mater. Rev.* **2013**, *56*, 143–166; b) Z. M. Sun, H. Hashimoto, Z. F. Zhang, S. L. Yang, S. Tada, *Mater. Trans.* **2006**, *47*, 170–174.

[3] M. W. Barsoum, M. Radovic, *Annu. Rev. Mater. Res.* **2011**, *41*, 195–227.

[4] a) M. W. Barsoum in *MAX Phases: Properties of Machinable Ternary Carbides and Nitrides*, Wiley-VCH, Weinheim, **2013**; b) M. W. Barsoum, D. Brodkin, T. El-Raghy, *Scr. Mater.* **1997**, *36*, 535–541.

[5] a) V. M. Hong Ng, H. Huang, K. Zhou, P. S. Lee, W. Que, J. Z. Xu, L. B. Kong, *J. Mater. Chem. A* **2017**, *5*, 3039–3068; b) M. Naguib, O. Mashtalir, J. Carle, V. Presser, J. Lu, L. Hultman, Y. Gogotsi, M. W. Barsoum, *ACS Nano* **2012**, *6*, 1322–1331; c) F. Shahzad, M. Alhabeb, C. B. Hatter, B. Anasori, S. Man Hong, C. M. Koo, Y. Gogotsi, *Science* **2016**, *353*, 1137; d) M. Ghidiu, M. R. Lukatskaya, M.-Q. Zhao, Y. Gogotsi, M. W. Barsoum, *Nature* **2014**, *516*, 78; e) M. R. Lukatskaya, O. Mashtalir, C. E. Ren, Y. Dall'Agnese, P. Rozier, P. L. Taberna, M. Naguib, P. Simon, M. W. Barsoum, Y. Gogotsi, *Science* **2013**, *341*, 1502; f) M. Naguib, V. N. Mochalin, M. W. Barsoum, Y. Gogotsi, *Adv. Mater.* **2014**, *26*, 992–1005; g) O. Mashtalir, M. Naguib, V. N. Mochalin, Y. Dall'Agnese, M. Heon, M. W. Barsoum, Y. Gogotsi, *Nat. Commun.* **2013**, *4*, 1716.

[6] M. Naguib, M. Kurtoglu, V. Presser, J. Lu, J. Niu, M. Heon, L. Hultman, Y. Gogotsi, M. W. Barsoum, *Adv. Mater.* **2011**, *23*, 4248–4253.

[7] O. Beckmann, H. Boller, H. Nowotny, *Monatsh. Chem.* **1968**, *99*, 1580–1583.

[8] a) W. Jeitschko, H. Nowotny, *Monatsh. Chem. Chem. Mon.* **1967**, *98*, 329–337; b) H. Wolfsgruber, H. Nowotny, F. Benesovsky, *Monatsh. Chem. Verw. Teile Anderer Wiss.* **1967**, *98*, 2403–2405.

[9] M. W. Barsoum, L. Farber, I. Levin, A. Procopio, T. El-Raghy, A. Berner, *J. Am. Ceram. Soc.* **1999**, *82*, 2545–2547.

[10] C. Hu, C. C. Lai, Q. Tao, J. Lu, J. Halim, L. Sun, J. Zhang, J. Yang, B. Anasori, J. Wang, Y. Sakka, L. Hultman, P. Eklund, J. Rosen, M. W. Barsoum, *Chem. Commun.* **2015**, *51*, 6560–6563.

[11] O. Beckmann, H. Boller, H. Nowotny, *Monatsh. Chem. Chem. Mon.* **1970**, *101*, 945–955.

[12] K. Sakamaki, H. Wada, H. Nozaki, Y. Ōnuki, M. Kawai, *J. Alloys Compd.* **2002**, *339*, 283–292.

[13] A. Altomare, C. Cuocci, C. Giacovazzo, A. Moliterni, R. Rizzi, N. Corriero, A. Falcicchio, *J. Appl. Crystallogr.* **2013**, *46*, 1231 – 1235.
[14] M. W. Barsoum, in *MAX Phases: Properties of Machinable Ternary Carbides and Nitrides*, Wiley-VCH, Weinheim, **2013**.
[15] a) T. Liao, J. Wang, Y. Zhou, *J. Phys. Condens. Matter* **2006**, *18*, L527 – L533; b) R. S. Kumar, S. Rekhi, A. L. Cornelius, M. W. Barsoum, *Appl. Phys. Lett.* **2005**, *86*, 111904; c) T. Liao, J. Wang, Y. Zhou, *J. Mater. Res.* **2011**, *24*, 556 – 564; d) S. R. Kulkarni, N. A. Phatak, S. K. Saxena, Y. Fei, J. Hu, *J. Phys. Condens. Matter* **2008**, *20*, 135211.
[16] a) S. R. Kulkarni, R. S. Vennila, N. A. Phatak, S. K. Saxena, C. S. Zha, T. El-Raghy, M. W. Barsoum, W. Luo, R. Ahuja, *J. Alloys Compd.* **2008**, *448*, L1 – L4; b) B. Manoun, R. P. Gulve, S. K. Saxena, S. Gupta, M. W. Barsoum, C. S. Zha, *Phys. Rev. B* **2006**, *73*, 024110; c) B. Manoun, H. P. Liermann, R. P. Gulve, S. K. Saxena, A. Ganguly, M. W. Barsoum, C. S. Zha, *Appl. Phys. Lett.* **2004**, *84*, 2799 – 2801.
[17] F. Birch, *J. Geophys. Res.: Solid Earth* **1978**, *83*, 1257 – 1268.
[18] B. Manoun, S. Saxena, T. El-Raghy, M. Barsoum, *Appl. Phys. Lett.* **2006**, *88*, 201902.
[19] M. W. Barsoum, *MAX Phases: Properties of Machinable Ternary Carbides and Nitrides*, Wiley-VCH, Weinheim, **2013**.
[20] Y. Medkour, A. Roumili, M. Boudissa, D. Maouche, L. Louail, A. Gamoura, *Comput. Mater. Sci.* **2010**, *48*, 174 – 178.
[21] M. F. Cover, O. Warschkow, M. Bilek, D. McKenzie, *J. Phys. Condens. Matter* **2009**, *21*, 305403.
[22] C. Hu, Y. Sakka, T. Nishimura, S. Guo, S. Grasso, H. Tanaka, *Science and Technology of Advanced Materials* **2011**, *12*, 044603.
[23] a) H. Boller, H. Nowotny, *Monatsh. Chem. Verw. Teile Anderer Wiss.* **1966**, *97*, 1053 – 1058; b) H. Boller, H. Nowotny, *Monatsh. Chem. Chem. Mon.* **1968**, *99*, 672 – 675.

Manuscript received: December 11, 2018
Accepted manuscript online: February 6, 2019
Version of record online: March 3, 2019

